Probing black hole accretion tracks, scaling relations, and radiative efficiencies from stacked X-ray active galactic nuclei

Francesco Shankar [1]⋆ David H. Weinberg,[2] Christopher Marsden,[1] Philip J. Grylls,[1] Mariangela Bernardi,[3] Guang Yang [4] Benjamin Moster [5] Hao Fu,[1] Rosamaria Carraro,[6] David M. Alexander,[7] Viola Allevato,[8] Tonima T. Ananna,[9] Angela Bongiorno,[10] Giorgio Calderone,[11] Francesca Civano,[12] Emanuele Daddi [13] Ivan Delvecchio,[13,14] Federica Duras [15] Fabio La Franca,[15] Andrea Lapi,[16] Youjun Lu,[17] Nicola Menci,[10] Mar Mezcua [18] Federica Ricci [19] Giulia Rodighiero,[20] Ravi K. Sheth,[3] Hyewon Suh,[21] Carolin Villforth[22] and Lorenzo Zanisi[1]

Affiliations are listed at the end of the paper

ABSTRACT

The masses of supermassive black holes at the centres of local galaxies appear to be tightly correlated with the mass and velocity dispersions of their galactic hosts. However, the local $M_{bh}-M_{star}$ relation inferred from dynamically measured inactive black holes is up to an order-of-magnitude higher than some estimates from active black holes, and recent work suggests that this discrepancy arises from selection bias on the sample of dynamical black hole mass measurements. In this work, we combine X-ray measurements of the mean black hole accretion luminosity as a function of stellar mass and redshift with empirical models of galaxy stellar mass growth, integrating over time to predict the evolving $M_{bh}-M_{star}$ relation. The implied relation is nearly independent of redshift, indicating that stellar and black hole masses grow, on average, at similar rates. Matching the de-biased local $M_{bh}-M_{star}$ relation requires a mean radiative efficiency $\varepsilon \gtrsim 0.15$, in line with theoretical expectations for accretion on to spinning black holes. However, matching the 'raw' observed relation for inactive black holes requires $\varepsilon \sim 0.02$, far below theoretical expectations. This result provides independent evidence for selection bias in dynamically estimated black hole masses, a conclusion that is robust to uncertainties in bolometric corrections, obscured active black hole fractions, and kinetic accretion efficiency. For our fiducial assumptions, they favour moderate-to-rapid spins of typical supermassive black holes, to achieve $\varepsilon \sim 0.12$–0.20. Our approach has similarities to the classic Soltan analysis, but by using galaxy-based data instead of integrated quantities we are able to focus on regimes where observational uncertainties are minimized.

Key words: black hole physics – galaxies: fundamental parameters – galaxies: nuclei – quasars: supermassive black holes – galaxies: star formation.

1 INTRODUCTION

Supermassive black holes are detected at the centres of almost all local galaxies observed with high enough sensitivity, and they seem to share close links with their host galaxies. The mass of central black holes is observed to scale proportionally with the stellar mass of the host galaxy and with the fourth or fifth power of its stellar velocity dispersion (e.g. Magorrian et al. 1998; Ferrarese & Merritt 2000; Häring & Rix 2004; Marconi et al. 2004; Kormendy & Ho 2013; Läsker et al. 2014; Graham & Scott 2015; van den Bosch et al. 2015; Savorgnan et al. 2016; Shankar et al. 2016a; Sahu, Graham & Davis 2019), suggesting a 'co-evolution' between the black holes and their hosts (e.g. Granato et al. 2004; Lapi et al. 2006; Shankar et al. 2006; Hopkins et al. 2008). In particular, from analysis of the residuals in the various scaling relations, evidence was put forwards that black hole mass M_{bh} is mostly correlated to velocity dispersion σ, rather than stellar mass M_{star} or any other galactic

⋆ E-mail: f.shankar@soton.ac.uk

property (e.g. Bernardi et al. 2007; Shankar, Bernardi & Sheth 2017; de Nicola, Marconi & Longo 2019; Shankar et al. 2019b), a possible signature of momentum/energetic feedback from the central black hole on their hosts during their bright phases as active galactic nuclei (AGNs; e.g. Silk & Rees 1998; King 2003; Fabian 2012; Zubovas & King 2019). In this context, a correlation between black hole mass and host galaxy (total) stellar mass would then be a by-product of the more fundamental $M_{bh}-\sigma$ and $\sigma-M_{star}$ relations.

Deciphering the origin and evolution of supermassive black holes in galaxies requires proper observational characterization of the black hole–galaxy scaling relations, which however remains a non-trivial challenge. One of the most pressing issues in this respect is the possible presence of observational biases affecting the scaling relations (e.g. Yu & Tremaine 2002; Batcheldor et al. 2007; Bernardi et al. 2007; Gültekin et al. 2011; Morabito & Dai 2012; Shankar et al. 2016a). Following the preliminary work by Bernardi et al. (2007), Shankar et al. (2016a) more recently emphasized that samples of local quiescent (mainly early type) galaxies having dynamically measured central black hole masses present larger velocity dispersions at fixed stellar mass with respect to the mean trend for early type galaxies in the Sloan Digital Sky Survey (SDSS). Via targeted Monte Carlo simulations in which black hole mass was assumed to scale as $M_{bh} \propto \sigma^{4-5}$, Shankar et al. (2016a) showed that the apparent discrepancies in the velocity distributions at fixed stellar mass could be straightforwardly explained in terms of an observational selection effect. To perform reliable dynamical black hole mass measurements, the black hole gravitational sphere of influence,[1] $r_g \propto M_{bh}/\sigma^2 \propto \sigma^\beta$ with $\beta \sim 2$–3, must be sufficiently resolved (e.g. Ferrarese & Ford 2005). The limited capabilities of present-day telescopes will inevitably favour the galaxies with the largest gravitational radii r_g, thus the highest velocity dispersions and highest black hole mass at fixed host galaxy stellar mass, biasing the observed scaling relations towards fictitiously higher normalizations. The Monte Carlo simulations showed that this gravitational bias by itself could account for the whole observed discrepancies in velocity dispersion distributions between SDSS galaxies and galaxies with dynamically measured black holes, whilst predicting biases up to an order of magnitude in the observed $M_{bh}-M_{star}$ relation. In what follows, we will always refer to the directly observed $M_{bh}-M_{star}$ relation as 'raw', and the claimed intrinsic $M_{bh}-M_{star}$ relation from Shankar et al. (2016a) as 'de-biased'. We will draw on additional observations and theoretical expectations of black hole accretion efficiency to argue that the de-biased relations are indeed more accurate. In a recent conference proceedings, Kormendy (2019) has argued that the scaling relations derived from dynamically measured black holes (e.g. Kormendy & Ho 2013) are not biased; we address each of the points raised in his article in the Appendix.

AGN samples with reverberation or single-epoch black hole mass estimates do not suffer from the restriction of needing to observationally resolve the (small) central black hole gravitational sphere of influence, as their black hole masses are retrieved from the virial product of the broad emission-line dispersions, which trace the gravitational potential in a region dominated by the black hole, and the radii inferred directly from reverberation mappings or indirectly from the size–luminosity relation (e.g. Peterson et al. 2004; Bentz

et al. 2008). If local AGN are random samples of the underlying population of dynamically measured supermassive black holes, they would be naturally expected to more closely trace the intrinsic/de-biased, rather than the observed/raw, $M_{bh}-M_{star}$ relation (Shankar et al. 2019b). Indeed, several groups found clear evidence for AGN to lie below the $M_{bh}-M_{star}$ relation of local, inactive black holes (e.g. Dasyra et al. 2007; Kim et al. 2008; Sarria et al. 2010; Busch et al. 2014; Falomo et al. 2014; Reines & Volonteri 2015; Greene et al. 2016; Ricci et al. 2017; Bentz & Manne-Nicholas 2018; Shankar et al. 2019b), when adopting virial factors $f_{vir} \sim 4$ as suggested by geometric and dynamic modelling of the broad-line region (e.g. Pancoast, Brewer & Treu 2014; Grier et al. 2017). More recently Shankar et al. (2019b) showed that the large-scale clustering as a function of black hole mass, as measured at $z = 0.25$ from large-scale optical and X-ray surveys by Krumpe et al. (2015), is fully consistent with the de-biased, rather than the raw, local $M_{bh}-M_{star}$ relation, further suggesting the presence of a bias in the latter.

The central aim of this work is to probe the shape, normalization and evolution of the relation between black hole mass and host galaxy (total) stellar mass $M_{bh}-M_{star}$ relation, in ways *independent* of the local sample of dynamically measured supermassive black holes. To this purpose, following the seminal works by Mullaney et al. (2012) and, in particular, Yang et al. (2018), we compute the $M_{bh}-M_{star}$ relation and its evolution with redshift adopting a new methodology that relies on large and deep X-ray AGN samples. More specifically, adopting the standard assumption that supermassive black holes are the relics of single or multiple gas accretion episodes in AGN (Lynden-Bell 1969; Soltan 1982; Rees 1984) and that their luminous outputs are regulated by a radiative efficiency ε (e.g. Bardeen, Press & Teukolsky 1972; Thorne 1974), we can directly convert the average AGN luminosities of a population of galaxies into the average mass accretion rates of their black holes $\langle \dot{M}_{BH,acc}\rangle[M_{star}(z), z] \propto \langle L_X[z, M_{star}(z)]\rangle/\varepsilon$. The average here includes those galaxies whose central black holes are inactive at a given time and thus contribute negligibly to the mean AGN luminosity.

By following the host stellar mass evolutionary tracks $M_{star}(z)$, derived from state-of-the-art semi-empirical models (e.g. Behroozi et al. 2019; Moster, Naab & White 2018; Grylls et al. 2019), we can integrate in time the mean accretion rate $\langle \dot{M}_{BH,acc}\rangle[M_{star}(z), z]$ to infer the mean black hole mass $\langle M_{bh}(z)\rangle$ at the centre of the host galaxy with average stellar mass $\langle M_{star}(z)\rangle$, and thus build the mean $\langle M_{bh}(z)\rangle-\langle M_{star}(z)\rangle$ relation at all accessible cosmic epochs (mostly $z \lesssim 3$). In our approach, it is irrelevant whether stellar mass is a primary or secondary galaxy property related to black hole mass, as it is simply adopted as a 'tracer' of the central AGN activity through cosmic time. Galaxy and black hole mergers are a potential complication to this approach but we will show that they should have little impact for the intermediate-mass galaxies from which we derive our main constraints.

We will show that the method outlined above produces $M_{bh}-M_{star}$ relations at the present epoch in close agreement with the de-biased $M_{bh}-M_{star}$ relation when adopting reasonable values of $\varepsilon \gtrsim 0.1$, as expected from standard accretion disc theory (Shakura & Sunyaev 1973) and as inferred from direct UV spectral energy distribution (SED) fitting (e.g. Davis & Laor 2011; Capellupo et al. 2015). On the other hand, matching the raw $M_{bh}-M_{star}$ relation would require unrealistically low radiative efficiencies of $\varepsilon \lesssim 0.04$. On the assumption of a time-invariant mean radiative efficiency, the results put forwards in this work also point to a constant $M_{bh}-M_{star}$ relation at all cosmic epochs probed by the stacked X-ray data, in line with recent independent estimates of the $M_{bh}-M_{star}$

[1]In the r_g formula in the text, the velocity dispersion is calculated at large scales, outside of the gravitational sphere of influence of the central black hole, and the constant of proportionality takes into account the galaxy profile. Discussions can be found in Shankar et al. (2016a) and Barausse et al. (2017).
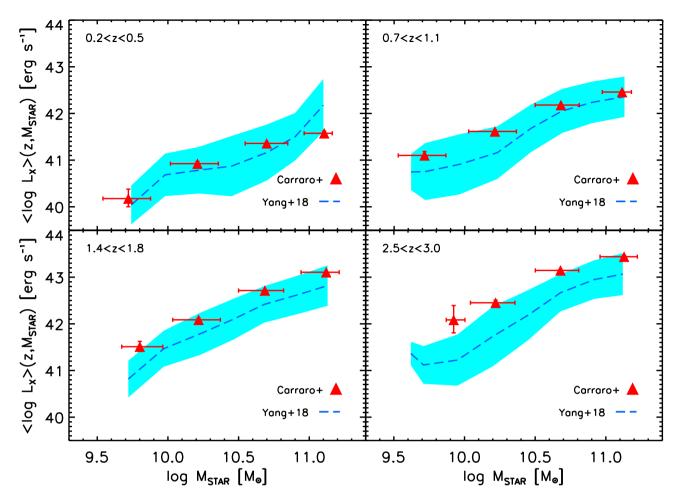
Figure 1. X-ray luminosities, averaged over active and inactive galaxies, as a function of stellar mass and redshift. Data are from Yang et al. (2018) and Carraro et al. (in preparation), as labelled. The cyan region brackets the 1σ scatter around the mean.

relation from high-redshift single-epoch AGN samples (Suh et al. 2020).

The method outlined in this work is similar in principle to the classical Soltan-type approach (Soltan 1982), in which the mean radiative efficiency ε is constrained by comparing the time-integrated accreted mass from (all) AGN, which scales with the (inverse) mean radiative efficiency, with the local supermassive black hole mass density or mass function (Salucci et al. 1999; Yu & Tremaine 2002; Marconi et al. 2004; Shankar et al. 2004; Yu & Lu 2008; Shankar, Weinberg & Miralda-Escudé 2009b; Shankar et al. 2013a; Aversa et al. 2015; Zhang & Lu 2017). A disadvantage of this classical approach is that it relies on integrated quantities, so it is sensitive to uncertainties at the extremes of the AGN luminosity function or black hole mass function (see e.g. Shankar 2009; Graham 2016 for reviews). The inference of the local black hole mass density is also sensitive to the uncertain scatter about the mean black hole–galaxy scaling relations. Whilst some systematic uncertainties also affect the approach used here, we are able to focus on specific regimes of galaxy mass and AGN luminosity where these uncertainties are minimized.

The paper is organized as follows. In Section 2, we briefly present the data we adopt as input to our calculations. Our methodology is then detailed in Section 3. We provide our results in Section 4 and conclude in Section 5. In what follows, wherever relevant we will adopt a reference cosmology with $h = 0.7$, $\Omega_m = 0.3$, $\Omega_\Lambda = 0.7$, and a Chabrier (2003) stellar initial mass function (IMF).

2 DATA

As our reference sample in this work we will make use of the X-ray luminosities from Yang et al. (2018), reported in Fig. 1. In brief, this sample of active and star-forming galaxies has been extracted from the GOODS North and South and COSMOS galaxy samples with stellar masses derived from SED fitting of broad-band photometry (Santini et al. 2015), cross-correlated with the Chandra Deep Fields North and South (see Yang et al. 2017, and references therein for full details), assuming a Chabrier (2003) IMF and mass-to-light ratios computed as median among different methods, including Bruzual & Charlot (2003) and Maraston (2005). Stellar masses in broad-line AGN were further corrected by Yang et al. (2018) to remove the AGN component. Adding contributions from AGN in passive galaxies at each stellar mass would change results only slightly (Yang et al. 2018).

Whilst Yang et al. (2018)'s reference IMF is the same as the one adopted in this paper, their mass-to-light ratios, especially those by Bruzual & Charlot (2003), may tend to provide less stellar mass than our reference Bell et al. (2003) value, at fixed galaxy luminosity or colour (Bell et al. 2003). Moreover, SED-based stellar masses may differ from photometrically based ones, such as those adopted by Savorgnan et al. (2016) and Shankar et al. (2016a) in deriving the host galaxy stellar masses of dynamically measured local black holes. To check for systematic differences in stellar mass estimates, we have cross-correlated the low-redshift galaxies in Laigle et al.

(2016), who make use of the SED-fitting technique and Bruzual & Charlot (2003) mass-to-light ratios on the COSMOS field, with the photometrically based stellar masses from the Meert, Vikram & Bernardi (2015) catalogue, which was adopted as a reference by Shankar et al. (2016a). We found the former to be, as expected, systematically smaller than the latter by a median of ∼0.15 dex. To be conservative, we do not apply such a correction in our final estimates, noticing that increasing the final stellar masses of Yang et al. (2018) at fixed black hole mass would if anything strengthen our main conclusions that reproducing the raw M_{bh}–M_{star} relation requires a very low radiative efficiency.

To check on the accuracy of the luminosities computed by Yang et al. (2018), we compare their average X-ray luminosities as a function of stellar mass in Fig. 1 (long-dashed, blue lines with cyan regions delimiting the 1σ uncertainties) with data from Carraro et al. (in preparation, red triangles), which have been extracted from Chandra stacking at 2–7 keV and converted to full band assuming $\Gamma = 1.8$. We find very good agreement between the independent samples, supporting the validity of the Yang et al. (2018) results. Averages in X-ray luminosity at a given stellar mass in Yang et al. (2018) are taken over the full population of galaxies, including galaxies with no AGN detection. They are computed by full integration of the double power-law probability distributions $P(L_X|M_{star}, z)$, which has been constrained from maximum-likelihood fitting by Yang et al. (2018). Such distributions have been shown, once convolved with the stellar mass function by Davidzon et al. (2017), to well reproduce the full X-ray luminosity function by Ueda et al. (2014) at any redshift of interest.

3 METHOD

We here outline the step-by-step methodology pursued in this work to build black hole mass accretion histories and constrain mean radiative efficiencies. Our aim is to provide a novel framework that broadly builds upon the classical Soltan (1982) argument, but also substantially expands beyond it making use of additional data and techniques. As visualized in Fig. 2, our approach consists of the following steps:

(i) We start from X-ray AGN luminosities converted to bolometric luminosities and averaged over the full populations of active and normal galaxies, and expressed as a function of stellar mass and redshift, $\langle L\rangle(M_{star}, z)$.

(ii) By assuming a mean radiative efficiency ε and kinetic efficiency ε_{kin}, we convert average AGN bolometric luminosities into mean black hole mass accretion rates

$$\langle \dot{M}_{BH,acc}\rangle(M_{star}, z) = \frac{\langle L\rangle(M_{star}, z)(1 - \varepsilon - \varepsilon_{kin})}{\varepsilon c^2}. \quad (1)$$

The factor $(1 - \varepsilon - \varepsilon_{kin})$ in equation (1) appears because ε is defined relative to the large-scale accretion rate, but energy emitted as radiation or kinetic feedback does not contribute to the black hole's mass growth.

(iii) We then make use of the mean galaxy mass accretion histories $M_{star}[z]$, inferred from extensive cosmological semi-empirical models built around the abundance matching technique, to predict the average growth rates of supermassive black holes $\langle \dot{M}_{BH,acc}\rangle(M_{star}[z], z)$. Average mass growth histories of supermassive black holes are then simply built by integrating $\langle \dot{M}_{BH,acc}\rangle(M_{star}[z], z)$ along cosmic time.

(iv) By integrating in redshift the galaxy and black hole mass accretion histories, we can retrieve the average black hole mass–stellar mass relation $\langle M_{bh}[z]\rangle - \langle M_{star}[z]\rangle$ at any redshift z of

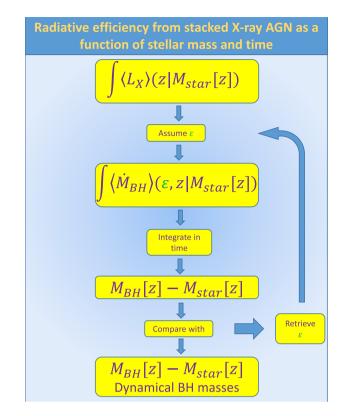**Figure 2.** Cartoon visualizing the strategy of this work. After assuming a constant radiative efficiency ε, average black hole accretion histories are extracted from the X-ray luminosities as a function of host galaxy stellar mass and redshift averaged over the entire active and non-active populations. We then follow input stellar mass growth histories $M_{star}[z]$, which are converted to black hole mass accretion histories via $L_x(z, M_{star})$ and ε. The comparison with the local dynamically based M_{bh}–M_{star} relations (or at any redshift $z < 2$ in which they are measured) can effectively constrain the input radiative efficiency, in ways largely independent of the obscured fraction of AGN (see the text for details).

interest.[2] The comparison with the latest determination of the local M_{bh}–M_{star} relation of dynamically measured supermassive black holes will then constrain the mean radiative efficiency.

The method outlined above is different from the traditional Soltan (1982) approach, as it does not deal with number densities but on mean accretion rates. It thus represents a novel, independent test of the connection between local black holes and distant AGN, and, as discussed below, it provides more robust constraints on the mean radiative efficiency of black holes. There are some key points important to emphasize at this stage. When comparing to a given rendition of the local M_{bh}–M_{star} relation, we are actually constraining the *ratio* between bolometric correction and radiative efficiency $k_{bol}(1 - \varepsilon - \varepsilon_{kin})/\varepsilon$. Nevertheless, we will see that within our current estimates of AGN bolometric corrections and obscured fractions, our proposed method provides a powerful test to bracket the allowed ranges of radiative efficiencies. We will also discuss the impact of allowing for additional kinetic losses in the estimate of the mean radiative efficiency.

---

[2]From now on, despite still referring to mean quantities throughout, we will usually drop the average symbols in black hole/galaxy stellar mass/accretion rates, for reasons of clarity.
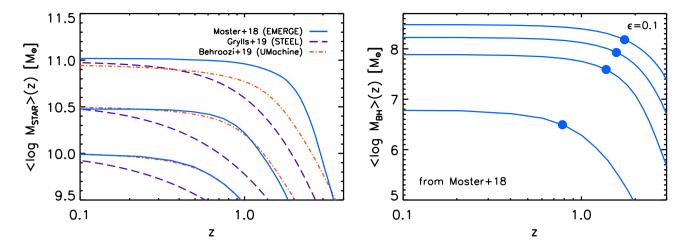
Figure 3. *Left*: Examples of average stellar mass growth histories $M_{star}[z]$ from Moster et al. (2018), Grylls et al. (2019), and Behroozi et al. (2019), as labelled. *Right*: Examples of average black hole mass accretion histories $M_{bh}[z]$ as expected from the mean X-ray luminosities of Fig. 1, assuming a radiative efficiency of $\varepsilon = 0.1$ and the Moster et al. (2018) stellar mass growth histories. The filled circle on each black hole mass track marks the redshift at which the black hole reaches 50 per cent of its final mass. Lower mass black holes gain more of their mass at late times, the behaviour often referred to as 'downsizing'.

4 RESULTS

4.1 Average black hole mass accretion histories

The first step of our modelling relies on computing reliable (average) X-ray luminosities as a function of stellar mass. As demonstrated by Yang et al. (2017) at fixed stellar mass, any secondary dependence of X-ray luminosities on star formation rates are weak. It is thus a good approximation in what follows to consider, at any redshift of interest, only an explicit dependence of X-ray luminosities on total stellar mass. We note that more recently Yang et al. (2019, see also Ni et al. 2019) found evidence for a strong connection between X-ray luminosity and star formation rate when considering only the bulge component. However, our methodology does not necessarily rely on any causal connection between star formation and AGN activity or X-ray luminosity on galaxy stellar mass. Stellar mass growth tracks are simply used as 'tracers' of AGN activity in our methodology, to connect descendants to progenitor AGN and thus estimate mean black hole accretion tracks.

X-ray luminosities averaged in small grids of redshift and stellar mass are then converted to average black hole accretion rates as follows:

$$\langle \dot{M}_{BH,acc} \rangle = \int_{-2}^{\infty} P(L_X | M_{star}, z) \frac{(1 - \varepsilon - \varepsilon_{kin}) k_{bol} L_X}{\varepsilon c^2} \, d \log L_X,$$

$$(2)$$

where k_{bol} is the bolometric correction adapted from Lusso et al. (2012, see fig. 8 in Yang et al. 2018). The lower limit of integration -2 corresponds to a minimum *specific* X-ray luminosity expressed in units of the host stellar mass. For a typical galaxy with mass $M_{star} = 10^{10} \, M_{\odot}$, this corresponds to an X-ray luminosity of $L_X \sim 4 \times 10^{41} \, \mathrm{erg \, s^{-1}}$ in the Yang et al. (2018) AGN samples, sufficient to probe down to the faint end of the X-ray AGN luminosity function (see Yang et al. 2018 for full details). Yang et al. (2018) performed additional tests to show that the cumulative black hole mass accreted at even lower specific X-ray luminosities is subdominant to the mass obtained via integration of equation (2). We also note that equation (2) strictly holds at $0.4 < z < 4$, though, as already noted by Yang et al. (2018), extending the validity of equation (2) to lower redshifts, as we do in this work, adds a minor contribution to the final black hole mass.

To compute black hole mass accretion histories, we thus need reliable estimates of how the host galaxies actually grow in stellar mass. We here neglect any source of '*ex situ*' accretion of stellar/black hole mass (e.g. mergers). This is a very good approximation as a number of cosmological analytic, semi-analytic, and numerical models (e.g. Shankar et al. 2013a; Rodriguez-Gomez et al. 2017; Lapi et al. 2018) agree in suggesting that the amount of stellar mass *ex situ* is limited to $\lesssim 20$ per cent for galaxies with $M_{star} \lesssim (1-2) \times 10^{11} \, M_{\odot}$. Moster et al. (2018), Lapi et al. (2018), and Grylls et al. (2020) have recently confirmed that, at least for the stellar mass range of interest to this work with $\log M_{star}/M_{\odot} \lesssim 11.2$, the cumulative accretion via satellite mergers is limited to a few per cent (see also Moster, Naab & White 2019).

The left-hand panel of Fig. 3 shows the Moster et al. (2018) semi-empirically constrained (EMERGE model) mean stellar mass growth histories of galaxies that today have a stellar mass of $\log M_{star}[z = 0]/M_{\odot} \sim 10, 10.5, 11$ (solid, blue lines), compared with another two recent semi-empirical models, the statistical model STEEL by Grylls et al. (2019, long-dashed purple lines), and the latest renditions of the UniverseMachine by Behroozi et al. (2019, dot–dashed, orange lines). All of these models are based on tracking backwards or forwards in time the host dark matter merger main progenitors, and at each time-step computing the mass gained in mergers and lost due to stellar evolution given an input stellar mass–halo mass relation tuned to specifically reproduce the local stellar mass function of Bernardi et al. (2013). This function is based on the same stellar mass system adopted by Shankar et al. (2016a, 2019b) to retrieve the M_{bh}–M_{star} relations adopted as a reference in this work. It is evident that despite being tuned against the same local stellar mass function, semi-empirical models may still produce noticeably distinct stellar mass growth tracks, with differences of up to 0.5 dex at any given epoch. The origin of these discrepancies can, at least in part, be reconciled to differences in the high-redshift input observational data adopted by each group. For example, Moster et al. (2018) tuned their model on larger star formation rates and lower stellar mass densities than those adopted in the STEEL reference model.

In what follows we will *conservatively* adopt as a reference the stellar mass growth tracks derived by Moster et al. (2018), noticing that our core conclusions would be similar, in fact strengthened, by switching to any other semi-empirical model among those reported
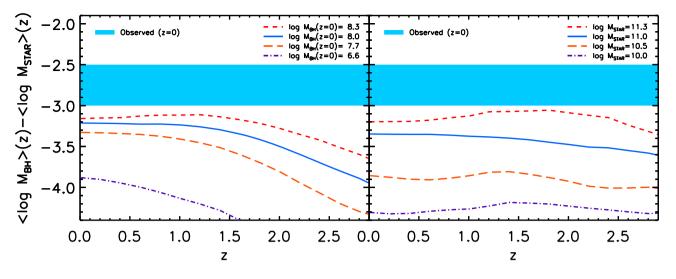
Figure 4. Examples of average black hole-to-stellar mass ratios as a function of redshift along the progenitors (left-hand panel) and at fixed stellar mass (right-hand panel), compared to the average ratio inferred by Kormendy & Ho (2013) in the local Universe (cyan region). At each M_{star} in the right-hand panel, the ratio $\langle M_{bh}\rangle/\langle M_{star}\rangle$ is roughly constant, at least for $z < 2$.

in the left-hand panel of Fig. 3. The Grylls et al. (2020) model, in particular, predicts steeper stellar mass growth histories which, at any given epoch, would correspond to moderately lower black hole accretion rates, which on average increase with host galaxy stellar mass (Yang et al. 2018). Steeper stellar mass growth histories would thus naturally lead to lower cumulative black hole masses and a proportionally lower normalization in the accreted $M_{bh}-M_{star}$ relation, at fixed radiative/kinetic efficiencies, bolometric correction, and obscured fraction. In turn, to match the raw $M_{bh}-M_{star}$ local relation, these steeper models would require mean radiative efficiencies lower than those, already quite extreme (see Section 4), implied by the Moster et al. (2018) stellar mass growth curves.

The right-hand panel of Fig. 3 shows the implied black hole mass accretion histories $\langle M_{bh}\rangle(M_{star}[z], z)$ obtained from direct time integration of the black hole accretion rates $\langle \dot{M}_{BH,acc}\rangle(M_{star}[z], z)$, included in Fig. 1, assuming a negligible kinetic efficiency and a nominal radiative efficiency of $\varepsilon = 0.1$. As mentioned above, we adopt the stellar mass growth tracks by Moster et al. (2018), and assume an initial black hole mass at $z = 4$ of $M_{star}/10^4$, sufficiently small to have a minor impact on the mass accreted at later epochs. As discussed by Yang et al. (2018), the choice of initial black hole mass has an overall negligible effect on the cumulative black hole masses at $z \lesssim 1.5$–2. The growth histories exhibit 'downsizing' – a shift towards growth of lower mass black holes at later times – which broadly mirrors the one in stellar mass reported in the left-hand panel of Fig. 3. We stress that the connection between black hole and stellar mass growth in Fig. 3 does not necessarily imply any causal connection between the two.

Fig. 4 depicts the ratio of the average black hole and stellar mass growth evolutionary histories, along the progenitor tracks $M_{star}[z]$ (left-hand panel), and at fixed stellar mass (right-hand panel), as labelled. It is interesting to see that, first off, the ratio $\langle M_{bh}[z]\rangle/\langle M_{star}[z]\rangle$ is not constant for all galaxies but it steadily decreases with decreasing stellar mass by up to an order of magnitude. Secondly, all ratios irrespective of redshift or stellar mass lie below the average black hole-to-stellar mass ratio inferred locally by Kormendy & Ho (2013, cyan region). Thirdly, all $\langle M_{bh}[z]\rangle/\langle M_{star}[z]\rangle$ ratios tend to remain roughly constant up until at least $z \sim 2$ at fixed stellar mass, in line with a number of previous studies, obtained via Monte Carlo approaches (Fiore et al. 2017), continuity equation

models (Shankar, Bernardi & Haiman 2009a; Zhang, Lu & Yu 2012; Shankar, Weinberg & Miralda-Escudé 2013b), integration of the star formation rate (Delvecchio et al. 2019), or direct observations (e.g. Gaskell 2009; Salviander & Shields 2013; Shen et al. 2015, see also Suh et al. 2020), all suggesting weak evolution in the black hole–galaxy scaling relations. On the other hand, the $\langle M_{bh}[z]\rangle/\langle M_{star}[z]\rangle$ ratios may tend to decrease at high redshifts, though this trend may be sensitive to the exact choice of initial black hole masses chosen at $z \gtrsim 4$, especially relevant in lower mass systems.

4.2 The comparison with the local $M_{bh}-M_{star}$ relation: towards constraining the mean radiative efficiency ε

Having devised robust methods to compute average stellar and black hole masses at any relevant epoch, we can compute the $M_{bh}-M_{star}$ relation in particular at $z \sim 0.1$ to compare with that independently inferred from local dynamical measures of supermassive black holes. Fig. 5 reports the latest renditions of the $M_{bh}-M_{star}$ relation. All data sets in Fig. 5 have been adjusted to the mass-to-light ratios adopted by Shankar et al. (2016a), based on Bell et al. (2003). We first apply a linear fit to the Kormendy & Ho (2013) local inactive sample dynamically measured supermassive black holes, as included in table 3 of Reines & Volonteri (2015), and correct stellar masses following equation A1 in Shankar et al. (2019b). The orange, triple dot–dashed line shows the linear fit by Sahu et al. (2019) to early-type galaxies, where we conservatively set the parameter $v = 1$ in their equation 11 (lower values of v, as suggested by Davis, Graham & Cameron 2018, would result in even higher normalizations). The raw $M_{bh}-M_{star}$ relation by Savorgnan et al. (2016), not reported in Fig. 5, is in broad agreement with the Kormendy & Ho (2013) relation (Shankar et al. 2019a).[3] The dashed green line shows the $M_{bh}-M_{star}$ relation inferred from

---

[3]For completeness, as already discussed by Shankar et al. (2019a), we also note that Davis et al. (2018) have recently inferred an $M_{bh}-M_{star}$ relation for local dynamically measured black holes hosted in late-type galaxies significantly steeper than the one by Sahu et al. (2019), roughly consistent with the Shankar et al. (2016a) estimate at $\log M_{star}/M_\odot \sim 10.5$, but rapidly approaching the Sahu et al. (2019) relation at $\log M_{star}/M_\odot \gtrsim 11$.
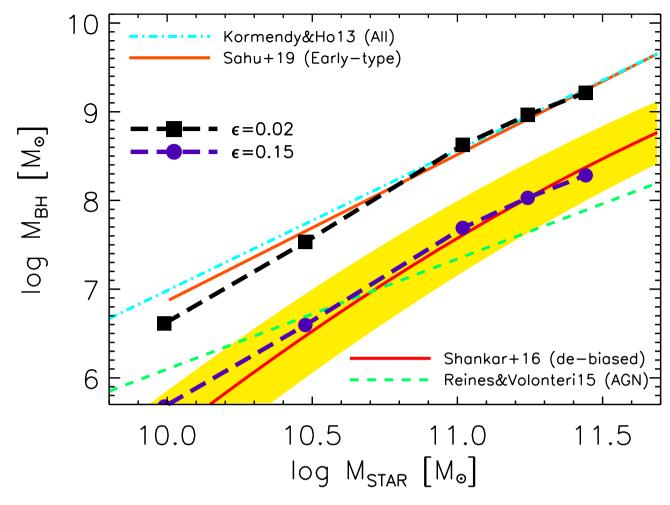
Figure 5. Correlations between central black hole mass and host galaxy *total* stellar mass in the local Universe. The triple dot–dashed orange line is the fit to the local quiescent sample of early-type galaxies with dynamical measures of black holes by Sahu et al. (2019). The dot–dashed, cyan line is a linear fit to the sample of Kormendy & Ho (2013). The solid red line with its scatter (yellow region) is the de-biased M_{bh}–M_{star} relation from Shankar et al. (2016a). The green dashed line is the fit to the local AGN from Reines & Volonteri (2015). Also included are the predicted average black hole mass as a function of host stellar mass at $z = 0.1$ for two different values of the radiative efficiency ε, as labelled. Values of $\varepsilon \sim 0.02$ are required (black long-dashed with filled squares) to match the normalization of the raw black hole M_{bh}–M_{star} relation for local dynamically measured quiescent black holes. A value of $\varepsilon \gtrsim 0.1$ is required (purple long-dashed with filled circles) to match the much lower M_{bh}–M_{star} relation inferred from AGN or the de-biased relation of Shankar et al. (2016a).

single-epoch black hole mass estimates for AGN host galaxies by Reines & Volonteri (2015, see also Baron & Ménard 2019; Shankar et al. 2019b), assuming a mean virial parameters $f_{vir} = 4.3$. In our terminology, the Kormendy & Ho (2013) and Sahu et al. (2019) relations are 'raw' estimates that fit the dynamically estimated black hole masses without accounting for the fact that this observed subset may be biased by the requirement of resolving the sphere of influence. The AGN sample is not subject to this bias, and the inferred M_{bh}–M_{star} relation is about an order-of-magnitude below the raw relations for inactive black holes at $M_{star} \sim 10^{11}\,M_\odot$.

As introduced in Section 1, Shankar et al. (2016a, see also Shankar et al. 2017, 2019b) confirmed earlier claims (Bernardi et al. 2007) that black hole mass pre-dominantly correlates with central stellar velocity dispersion σ, with all other scaling relations with black hole mass being mostly driven by the former one. We focus here on the M_{bh}–M_{star} relation because the higher redshift mean accretion rates are available as a function of stellar mass (Yang et al. 2018) rather than σ, which is more difficult to measure. Using mock black hole samples that follow an M_{bh}–σ relation and the σ–M_{star} relation of SDSS early-type galaxies, Shankar et al.

(2016a) derived a de-biased M_{bh}–M_{star} relation, valid for galaxies with $M_{star} \gtrsim 2 \times 10^{10}\,M_\odot$, which is shown by the red curve in Fig. 5, with the yellow band showing the inferred 1σ scatter of M_{bh} at fixed M_{star}. Including contributions from later-type galaxies would tend to produce slightly lower normalizations of the global unbiased M_{bh}–M_{star} relation (Shankar et al. 2019b). In principle, the discrepancy between the raw M_{bh}–M_{star} relations for quiescent black holes and the Reines & Volonteri (2015) result for AGN could arise because active galaxies have lower mass black holes, or because the virial factors used by Reines & Volonteri (2015) are much too low. However, a more natural interpretation of Fig. 5 is that the de-biased M_{bh}–M_{star} relation of Shankar et al. (2016a) is a better tracer of the mean M_{bh}–M_{star} scaling relation, that active galaxies host black holes similar to those of other galaxies with the same stellar mass, and that virial factors are in line with theoretical expectations and empirically constrained models of the broad-line region. This argument and its implications are explored in greater detail by Shankar et al. (2019b).

Fig. 5 presents an entirely independent argument for this point of view. Reproducing the raw M_{bh}–M_{star} relation with our empirically
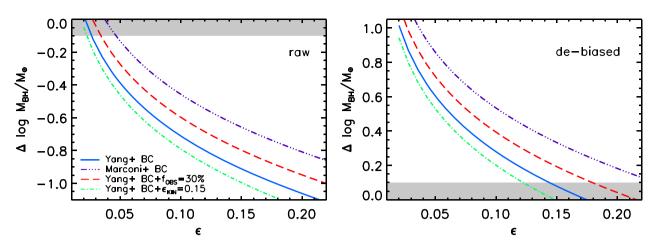
Figure 6. *Left*: Displacement $\Delta \log M_{bh}$ between the $\log M_{bh}$–$\log M_{star}$ relations of Kormendy & Ho (2013) and the one inferred from direct integration of the black hole accretion rate. *Right*: Displacement in $\log M_{bh}$ between the $\log M_{bh}$–$\log M_{star}$ relations of Shankar et al. (2016a) and the one inferred from direct integration of the black hole accretion rate. The solid blue, long-dashed red, triple dot–dashed purple, and green dot–dashed lines refer, respectively, to models based on the bolometric correction by Yang et al. (2018), on the bolometric correction by Marconi et al. (2004), the bolometric correction by Yang et al. (2018) plus some correction for obscured sources, and on the bolometric correction by Yang et al. (2018) plus a kinetic efficiency of $\varepsilon_{kin} = 0.15$. Higher bolometric corrections or significant obscured fractions require larger radiative efficiencies to reproduce the de-biased M_{bh}–M_{star} relation.

based models of Section 4.1 requires a radiative efficiency $\varepsilon \sim 0.02$ (black dashed curve), well below the value expected from accretion disc theory (e.g. Shakura & Sunyaev 1973; Abramowicz & Fragile 2013). Reproducing the de-biased or AGN relation requires $\varepsilon \sim 0.15$ (purple dashed curve), in good agreement with theoretical predictions for accretion on to spinning black holes. This agreement between the de-biased local M_{bh}–M_{star} relation and the prediction of a theoretically motivated, empirically based model is the principal result of this paper.

4.3 The impact of systematics and robustness of results

Although empirically based, our strategy still relies on a few input parameters and/or assumptions. In this section, we will detail how our main results are robust against sensible variations of such inputs. First off, the masses of supermassive black holes obtained by direct integration of equation (2) require specification of the bolometric correction. Following Yang et al. (2018), in Fig. 5 we have adopted as a reference the bolometric correction determined by Lusso et al. (2012). Other bolometric corrections proposed in the literature are characterized by up to factor of ∼3 higher normalizations (e.g. Marconi et al. 2004; Hopkins et al. 2006). This will proportionally increase the integrated emissivity of AGN and thus the predicted final black hole mass at fixed stellar mass. Lining up to the same local M_{bh}–M_{star} relation will therefore require a nearly proportional increase in the mean radiative efficiency ε, as one can see from the appearance of the ratio k_{bol}/ε in equation (2). Another important point is that the average X-ray luminosities adopted in equation (2) and taken from Yang et al. (2018) do not necessarily account for possible additional large populations of hidden Compton-thick AGN. If present, the latter would clearly increase the total intrinsic X-ray luminosities and thus the black hole accretion rates and predicted final masses, at fixed stellar mass, bolometric correction, and radiative efficiency. On the other hand, allowing for a non-negligible kinetic efficiency ε_{kin} as expected from studies of radio-loud AGN (Merloni & Heinz 2007; Shankar et al. 2008; La Franca, Melini & Fiore 2010; Ghisellini et al. 2013; Zubovas 2018) would tend to decrease the required mean radiative efficiency, when fixing the other parameters.

We summarize these behaviours in Fig. 6. The solid blue, triple dot–dashed purple, long-dashed red, and green dot–dashed lines refer, respectively, to models based (see equation 2) on the bolometric correction by Yang et al. (2018), on the bolometric correction by Marconi et al. (2004), on the bolometric correction by Yang et al. (2018) plus an additional multiplicative factor of 1.3 in equation (2) to account for possible underestimates of the total mean intrinsic X-ray luminosity due to missed Compton-thick AGN (e.g. Ueda et al. 2014; Harrison et al. 2016; Ananna et al. 2019; Georgantopoulos & Akylas 2019), and on the bolometric correction by Yang et al. (2018) plus a kinetic efficiency of $\varepsilon_{kin} = 0.15$. The left-hand panel shows the displacement, at a reference stellar mass of $\log M_{star}/M_\odot = 11$, in $\log M_{bh}$ between the $\log M_{bh}$–$\log M_{star}$ relation of Kormendy & Ho (2013) and the one inferred from direct integration of the black hole accretion rate. The right-hand panel shows the same quantity for the de-biased relation of Shankar et al. (2016a). Adopting the higher bolometric correction or the additional 30 per cent obscured accretion fraction increases the implied radiative efficiency, but we would still require $\varepsilon \lesssim 0.04$ to reproduce the raw M_{bh}–M_{star} relation to within 0.1 dex. The latest recalibration of the hard X-ray AGN bolometric corrections (Duras et al. 2020) tends to disfavour 'higher' bolometric corrections (Marconi et al. 2004; Hopkins, Richards & Hernquist 2007) and well align with those determined by Lusso et al. (2012).

It is worth emphasizing that throughout this work we are, by design, dealing with mean radiative efficiencies modelled via the thin-disc approximation (Shakura & Sunyaev 1973). Broad distributions of radiative efficiencies are indeed expected (e.g. Zhang & Lu 2017). In particular, substantial portions of the black hole population accreting at very low radiative efficiencies could be missed in our modelling. As discussed by Yang et al. (2018, and references therein), very low radiative efficiencies, significantly below the thin-disc approximation, for example in ADAF-like states, are expected to become effective only in extremely low Eddington ratio regimes (below 1 per cent of the Eddington limit). Such accretion mode is however too slow to provide a visible contribution to the final black holes, building mass on e-folding time-scales much longer than the Hubble time (see Yang et al. 2018 for further details).

5 CONCLUSIONS

As sketched in Fig. 2, we have put forwards a complementary approach to the classical Soltan (1982) method, taking advantage of recent measurements of the average X-ray luminosity of accreting black holes as a function of galaxy stellar mass and redshift (Yang et al. 2018), and of recent empirical models for the evolution of galaxy stellar masses (Moster et al. 2018). For an assumed mean radiative efficiency ε, these empirical inputs allow us to predict the mean M_{bh}–M_{star} relation as a function of redshift. We focus on the mass range log $M_{star}/M_\odot \sim 10.5$–11.2, where mergers are expected to be minor contributors to stellar mass and black hole growth (e.g. Shankar et al. 2013b; Lapi et al. 2018; Moster et al. 2018; and references therein). Assuming constant radiative efficiency, we infer (Fig. 4) that the normalization and shape of the M_{bh}–M_{star} relation is nearly independent of redshift at least up to $z \sim 2$, in agreement with the findings of Yang et al. (2018). Weak or negligible evolution of the M_{bh}–σ relation has been inferred from analysis based on the black hole continuity equation (Shankar et al. 2009a) and from some direct observational studies (Gaskell 2009; Shen et al. 2015). A non-evolving M_{bh}–M_{star} relation implies that the stellar masses and central black hole masses of galaxies grow, on average, at the same rate over cosmic time. A non-evolving M_{bh}–M_{star} and M_{bh}–σ relations would also imply weak evolutions in the σ–M_{star} relations and in the overall Fundamental Plane of massive galaxies and their central black holes (see e.g. discussion in Suh et al. 2020).

Most importantly, we find (Fig. 5) that reproducing the raw observed relation between galaxy stellar masses and the dynamically inferred masses of inactive black holes requires a radiative efficiency $\varepsilon \sim 0.02$, well below theoretical expectations for thin accretion discs and values inferred from UV SED fitting (e.g. Davis & Laor 2011; Trakhtenbrot 2014; Capellupo et al. 2015; Shankar et al. 2016b) and X-ray reflection analysis (Reynolds 2014). Higher bolometric corrections or significant fractions of obscured accretion can increase the inferred ε, but we still find $\varepsilon \lesssim 0.05$ for reasonable assumptions about these uncertainties (Fig. 6). This mismatch between the inferred ε and physical expectations provides independent evidence that the raw M_{bh}–M_{star} relation for inactive black holes is biased high because black hole masses are only measured when the radius of gravitational influence is resolved, as argued by Shankar et al. (2016a). Using Shankar et al. (2016a)'s de-biased M_{bh}–M_{star} relation, or the relation inferred from AGN black hole mass estimates by Reines & Volonteri (2015), we find a mean radiative efficiency $\varepsilon \sim 0.15$, in good agreement with theoretical expectations for accretion on to black holes with spin parameters $a \sim 0.5$–1. The red solid line in Fig. 7 shows the monotonic dependence of the spin parameter on radiative efficiency, obtained by integrating the specific energy and orbital angular momentum equations in the limit (Bardeen et al. 1972; Zhang & Lu 2019) of no kinetic loss $\varepsilon = 1 - E(R_{isco})$, with $E(R_{isco})$ the specific orbital energy at the innermost stable circular orbit with radius R_{isco}. This model suggests that values of $a \gtrsim 0.5$ would correspond to radiative efficiencies greater than $\varepsilon \gtrsim 0.1$ (black arrows in Fig. 7), which would be in line with the limits on ε obtained in this work when comparing with the de-biased M_{bh}–M_{star} relations (purple area in the upper right of Fig. 7), but in tension with the allowed ranges of ε required by the match to the raw M_{bh}–M_{star} relations (cyan area in the bottom left of Fig. 7). Flux limit effects may bias current X-ray surveys towards higher luminosity sources, possibly characterized by larger radiative efficiencies/spins (Vasudevan et al. 2016, see also Gandhi et al. 2007). As mentioned in Shankar et al. (2019a), the lower limits on the current AGN X-ray samples map to black holes radiating down to minimal radiative
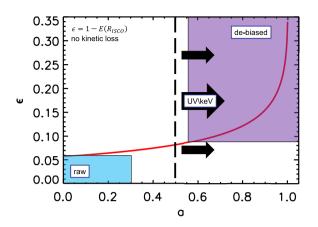

Figure 7. Radiative efficiency as a function of black hole spin (solid, red line) for direct accretion assuming no kinetic losses and $\varepsilon = 1 - E$ with E the energy at the innermost stable circular orbit (Bardeen et al. 1972). The constraints on the mean radiative efficiency arising from the fit to the intrinsic/unbiased M_{bh}–M_{star} relation, $\varepsilon \gtrsim 0.1$ (with dimensionless spin parameter $a \gtrsim 0.5$), are shown with a purple rectangle, whilst those from the observed M_{bh}–M_{star} relation, $\varepsilon \lesssim 0.05$, are shown with a cyan rectangle. The independent estimates of the spin parameter from UV/X-ray spectral modelling (black arrows) are broadly consistent with the former estimates with $a \gtrsim 0.5$.

efficiencies of $\varepsilon \sim 0.05$ and accreting at $\gtrsim 10$ per cent the Eddington limit, well within the thin-disc limit during which most of the final black hole mass is expected to assemble (Yang et al. 2018).

Uncertainties in bolometric corrections, kinetic feedback efficiency, and other observational inputs are large enough that we cannot clearly rule out efficiencies $\epsilon < 0.1$ achievable with non-spinning black holes, though models would still require relatively high ε_{kin} to accommodate very low radiative efficiencies (Fig. 6). A non-negligible obscured AGN fraction f for galaxies in our stellar mass range (e.g. Harrison et al. 2016; Ananna et al. 2019) would increase our inferred ε by a factor of $\sim(1 + f)$, so at face value our results favour $\varepsilon \gtrsim 0.15$–0.20, implying high characteristic spin parameters $a \gtrsim 0.9$. Most direct measurements of black hole spins from X-ray reflection spectroscopy favour $a \gtrsim 0.5$ (see e.g. table 1 in Zhang & Lu 2019), a finding further corroborated by UV SED modelling (e.g. Capellupo et al. 2015; Shankar et al. 2016b). Future observations and modelling can reduce uncertainties in bolometric corrections and the contribution of obscured accretion. They can also test our predictions against direct observations of the (non)-evolving M_{bh}–M_{star} relation (Suh et al. 2020), AGN and quasar clustering (e.g. Shankar, Weinberg & Shen 2010), and the cross-correlation of AGN and galaxies (e.g. Krumpe et al. 2015).

REFERENCES

Abramowicz M. A., Fragile P. C., 2013, Living Rev. Relativ., 16, 1

Ananna T. T. et al., 2019, ApJ, 871, 240

Aversa R., Lapi A., de Zotti G., Shankar F., Danese L., 2015, ApJ, 810, 74

Barausse E., Shankar F., Bernardi M., Dubois Y., Sheth R. K., 2017, MNRAS, 468, 4782

Bardeen J. M., Press W. H., Teukolsky S. A., 1972, ApJ, 178, 347

Baron D., Ménard B., 2019, MNRAS, 487, 3404

Batcheldor D., Marconi A., Merritt D., Axon D. J., 2007, ApJ, 663, L85

Behroozi P., Wechsler R., Hearin A., Conroy C., 2019, MNRAS, 488, 3143

Bell E. F., McIntosh D. H., Katz N., Weinberg M. D., 2003, ApJ, 149, S289

Bentz M. C., Manne-Nicholas E., 2018, ApJ, 864, 146

Bentz M. C., Peterson B. M., Netzer H., Pogge R. W., Vestergaard M., 2009, ApJ, 697, 160

Bernardi M., Sheth R. K., Tundo E., Hyde J. B., 2007, ApJ, 660, 267

Bernardi M., Meert A., Sheth R. K., Vikram V., Huertas-Company M., Mei S., Shankar F., 2013, MNRAS, 436, 697

Bruzual G., Charlot S., 2003, MNRAS, 344, 1000

Busch G. et al., 2014, A&A, 561, A140

Busch G. et al., 2016, A&A, 587, A138

Capellupo D. M., Netzer H., Lira P., Trakhtenbrot B., Mejía-Restrepo J., 2015, MNRAS, 446, 3427

Chabrier G., 2003, PASP, 115, 763

Dasyra K. M. et al., 2007, ApJ, 657, 102

Davidzon I. et al., 2017, A&A, 605, A70

Davis B. L., Graham A. W., Cameron E., 2018, ApJ, 869, 113

Davis S. W., Laor A., 2011, ApJ, 728, 98

Delvecchio I. et al., 2019, ApJ, 885, L36

de Nicola S., Marconi A., Longo G., 2019, MNRAS, 490, 600

Duras F. et al., 2020, MNRAS, preprint (arXiv:2001.09984)

Fabian A. C., 2012, ARA&A, 50, 455

Falomo R., Bettoni D., Karhunen K., Kotilainen J. K., Uslenghi M., 2014, MNRAS, 440, 476

Ferrarese L., Ford H., 2005, Space Sci. Rev., 116, 523

Ferrarese L., Merritt D., 2000, ApJ, 539, L9

Fiore F. et al., 2017, A&A, 601, A143

Gandhi P., Fabian A. C., Suebsuwong T., Malzac J., Miniutti G., Wilman R. J., 2007, MNRAS, 382, 1005

Gaskell C. M., 2009, preprint (arXiv:0908.0328)

Georgantopoulos I., Akylas A., 2019, A&A, 621, A28

Ghisellini G., Haardt F., Della Ceca R., Volonteri M., Sbarrato T., 2013, MNRAS, 432, 2818

Graham A. W., 2016, Galactic Bulges, 418, 263

Graham A. W., Scott N., 2015, ApJ, 798, 54

Granato G. L., De Zotti G., Silva L., Bressan A., Danese L., 2004, ApJ, 600, 580

Greene J. E. et al., 2016, ApJ, 826, L32

Grier C. J., Pancoast A., Barth A. J., Fausnaugh M. M., Brewer B. J., Treu T., Peterson B. M., 2017, ApJ, 849, 146

Grylls P. J., Shankar F., Zanisi L., Bernardi M., 2019, MNRAS, 483, 2506

Grylls P. J., Shankar F., Leja J., Menci N., Moster B., Behroozi P., Zanisi L., 2020, MNRAS, 491, 634

Gültekin K., Tremaine S., Loeb A., Richstone D. O., 2011, ApJ, 738, 17

Häring N., Rix H.-W., 2004, ApJ, 604, L89

Harrison F. A. et al., 2016, ApJ, 831, 185

Hopkins P. F., Hernquist L., Cox T. J., Robertson B., Di Matteo T., Springel V., 2006, ApJ, 639, 700

Hopkins P. F., Richards G. T., Hernquist L., 2007, ApJ, 654, 731

Hopkins P. F., Hernquist L., Cox T. J., Kereš D., 2008, ApJS, 175, 356

Kim M., Ho L. C., Peng C. Y., Barth A. J., Im M., Martini P., Nelson C. H., 2008, ApJ, 687, 767

King A., 2003, ApJ, 596, L27

Kormendy J., 2019, preprint (arXiv:1909.10821)

Kormendy J., Bender R., 2013, ApJ, 769, L5

Kormendy J., Ho L. C., 2013, ARA&A, 51, 511

Krumpe M., Miyaji T., Husemann B., Fanidakis N., Coil A. L., Aceves H., 2015, ApJ, 815, 21

La Franca F., Melini G., Fiore F., 2010, ApJ, 718, 368

Laigle C. et al., 2016, ApJS, 224, 24

Lapi A., Shankar F., Mao J., Granato G. L., Silva L., De Zotti G., Danese L., 2006, ApJ, 650, 42

Lapi A. et al., 2018, ApJ, 857, 22

Läsker R., Ferrarese L., van de Ven G., Shankar F., 2014, ApJ, 780, 70

Lauer T. R. et al., 2007, ApJ, 662, 808

Lusso E. et al., 2012, MNRAS, 425, 623

Lynden-Bell D., 1969, Nature, 223, 690

Magorrian J. et al., 1998, AJ, 115, 2285

Maraston C., 2005, MNRAS, 362, 799

Marconi A., Risaliti G., Gilli R., Hunt L. K., Maiolino R., Salvati M., 2004, MNRAS, 351, 169

Meert A., Vikram V., Bernardi M., 2015, MNRAS, 446, 3943

Merloni A., Heinz S., 2007, MNRAS, 381, 589

Morabito L. K., Dai X., 2012, ApJ, 757, 172

Moster B. P., Naab T., White S. D. M., 2018, MNRAS, 477, 1822

Moster B. P., Naab T., White S. D. M., 2019, preprint (arXiv:1910.09552)

Mullaney J. R. et al., 2012, ApJ, 753, L30

Ni Q., Yang G., Brandt W. N., Alexander D. M., Chen C. T. J., Luo B., Vito F., Xue Y. Q., 2019, MNRAS, 490, 1135

Pancoast A., Brewer B. J., Treu T., 2014, MNRAS, 445, 3055

Peterson B. M. et al., 2004, ApJ, 613, 682

Rees M. J., 1984, ARA&A, 22, 471

Reines A. E., Volonteri M., 2015, ApJ, 813, 82

Reynolds C. S., 2014, Space Sci. Rev., 183, 277

Ricci F. et al., 2017, MNRAS, 471, L41

Rodriguez-Gomez V. et al., 2017, MNRAS, 467, 3083

Sahu N., Graham A. W., Davis B. L., 2019, ApJ, 876, 155

Salucci P., Szuszkiewicz E., Monaco P., Danese L., 1999, MNRAS, 307, 637

Salviander S., Shields G. A., 2013, ApJ, 764, 80

Santini P. et al., 2015, ApJ, 801, 97

Sarria J. E., Maiolino R., La Franca F., Pozzi F., Fiore F., Marconi A., Vignali C., Comastri A., 2010, A&A, 522, L3

Savorgnan G. A. D., Graham A. W., Marconi A., Sani E., 2016, ApJ, 817, 21

Shakura N. I., Sunyaev R. A., 1973, A&A, 24, 337

Shankar F., 2009, New Astron. Rev., 53, 57

Shankar F., Salucci P., Granato G. L., De Zotti G., Danese L., 2004, MNRAS, 354, 1020

Shankar F., Lapi A., Salucci P., De Zotti G., Danese L., 2006, ApJ, 643, 14

Shankar F., Cavaliere A., Cirasuolo M., Maraschi L., 2008, ApJ, 676, 131

Shankar F., Bernardi M., Haiman Z., 2009a, ApJ, 694, 867

Shankar F., Weinberg D. H., Miralda-Escudé J., 2009b, ApJ, 690, 20

Shankar F., Weinberg D. H., Shen Y., 2010, MNRAS, 406, 1959

Shankar F., Marulli F., Bernardi M., Mei S., Meert A., Vikram V., 2013a, MNRAS, 428, 109

Shankar F., Weinberg D. H., Miralda-Escudé J., 2013b, MNRAS, 428, 421

Shankar F. et al., 2016a, MNRAS, 460, 3119

Shankar F. et al., 2016b, ApJ, 818, L1

Shankar F., Bernardi M., Sheth R. K., 2017, MNRAS, 466, 4029

Shankar F. et al., 2019a, NatAs, preprint (arXiv:1910.10175)

Shankar F. et al., 2019b, MNRAS, 485, 1278

Shen Y. et al., 2015, ApJ, 805, 96

Silk J., Rees M. J., 1998, A&A, 331, L1

Soltan A., 1982, MNRAS, 200, 115

Suh H., Civano F., Trakhtenbrot B., Shankar F., Hasinger G., Sanders D. B., Allevato V., 2020, ApJ, 889, 32

Thorne K. S., 1974, ApJ, 191, 507

Trakhtenbrot B., 2014, ApJ, 789, L9

Ueda Y., Akiyama M., Hasinger G., Miyaji T., Watson M. G., 2014, ApJ, 786, 104

van den Bosch R. C. E., Gebhardt K., Gültekin K., Yıldırım A., Walsh J. L., 2015, ApJS, 218, 10

Vasudevan R. V., Fabian A. C., Reynolds C. S., Aird J., Dauser T., Gallo L. C., 2016, MNRAS, 458, 2012

Yang G. et al., 2017, ApJ, 842, 72

Yang G. et al., 2018, MNRAS, 475, 1887

Yang G., Brandt W. N., Alexander D. M., Chen C. T. J., Ni Q., Vito F., Zhu F. F., 2019, MNRAS, 485, 3721

Yu Q., Lu Y., 2008, ApJ, 689, 732

Yu Q., Tremaine S., 2002, MNRAS, 335, 965

Zhang X., Lu Y., 2017, Sci. China Phys. Mech. Astron., 60, 109511

Zhang X., Lu Y., 2019, ApJ, 873, 101

Zhang X., Lu Y., Yu Q., 2012, ApJ, 761, 5

Zubovas K., 2018, MNRAS, 479, 3189

Zubovas K., King A. R., 2019, Gen. Relativ. Gravit., 51, 65

APPENDIX: THE IMPACT OF REDSHIFT AND APERTURE

In a very recent proceeding of the IAU Symposium 2019, Kormendy (2019) stated that local scaling relations of dynamically measured black holes are not biased. In this appendix, we carefully address this statement in light of his data and addressing some of his concerns. In our assessment, the bias in the black hole scaling relations that we have identified in our previous papers is fully consistent with the data recently presented by Kormendy (2019).

Kormendy (2019) first of all notices that the host galaxies of dynamically measured black holes follow the same scaling relations traced by larger serendipitous samples of local galaxies (e.g. fig. 1). Shankar et al. (2016a, 2017) have indeed demonstrated that, when compared to local SDSS galaxies, most scaling relations in terms of effective radius, Sérsic index, and dynamical mass are very similar for galaxies with and without central black hole dynamical mass measurement. Shankar et al. (2016a, 2017, 2019b) following Bernardi et al. (2007) highlighted that the bias is mostly evident in the velocity dispersion distributions at fixed stellar mass. The hosts of supermassive black holes tend to have mean velocity dispersions, on average, systematically higher by ∼0.05–0.2 dex, with the discrepancy gradually increasing towards lower stellar masses, than SDSS galaxies. Although this discrepancy is apparently relatively small, it could generate offsets in mean black hole masses up to a factor of ∼2–10, on the assumptions that black hole mass is primarily related to velocity dispersion scaling as $M_{\rm bh} \propto \sigma^5$, as suggested by residuals analysis (Bernardi et al. 2007; Shankar et al. 2016a; Shankar et al. 2017, 2019b) and the study of mono- and bivariate correlations (de Nicola et al. 2019). It is important to note that the analysis of Shankar et al. (2016a, 2017) is based on the Savorgnan et al. (2016) sample of *early-type* galaxies with dynamical black hole mass measurement, which was for full consistency compared with only early-type SDSS galaxies, with minimal contribution from pseudo-bulges (Shankar et al. 2016a, 2017). Shankar et al. (2019b) further extended the comparison between spirals in the SDSS galaxies and the (few) spirals in the Savorgnan et al. (2016) sample, showing that for black holes hosted in spirals the bias in mean velocity dispersion at fixed total stellar mass persists but it is less evident.

Kormendy (2019) attempts in fig. 2 a similar comparison between velocity dispersion and total galaxy magnitude in *V* band for local galaxies with black holes, and the broken power-law velocity dispersion–absolute magnitude scaling relation of local galaxies from Lauer et al. (2007) and Kormendy & Bender (2013). We propose a similar comparison in Fig. A1 in which we linearly fit his sample of galaxies with black holes (cyan long-dashed line) and compare it with his quoted velocity dispersion-absolute magnitude relation (black solid line). It is apparent that the mean
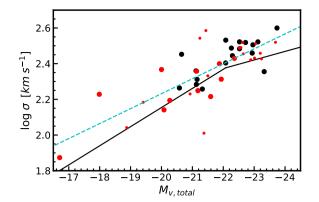

Figure A1. Same layout as fig. 2 in Kormendy (2019). Comparison between the double power-law local σ–M_V relation (solid black line) by Lauer et al. (2007) and Kormendy & Bender (2013), with the Kormendy (2019) data set of galaxies with dynamical measurements of their central supermassive black hole mass subdivided into core (black circles) and coreless (red circles) galaxies. The long-dashed, cyan line is a linear fit to the Kormendy (2019) black hole data, proving that at fixed (total) galaxy magnitude M_V, local black holes' hosts tend to have larger mean velocity dispersions than the underlying population of local galaxies.

velocity dispersion in the Kormendy (2019) black hole sample still presents an offset of ∼0.05–0.2 dex at fixed galaxy magnitude, increasing with decreasing galaxy luminosity. Indeed, Kormendy (2019) recognizes that velocity dispersions in his sample tend to lie above the mean velocity dispersion–absolute magnitude relation of local galaxies, and also addresses the issue of incompleteness in the local sample of black holes, as more distant galaxies have not been searched for. The offset between the two relations in Fig. A1 appears small, but it is enough to cause a large bias in the $M_{\rm bh}$–$M_{\rm star}$ relation because the $M_{\rm bh}$–σ relation is so steep.

Last but not least, Kormendy (2019) highlights the possible bias inherent in the SDSS survey dominated by more distant galaxies. Fixed apertures would naturally sample larger radii of the galaxies and possibly measure lower velocity dispersions at fixed stellar mass. To check for this possible aperture-distance effect, we have analysed 2000 early-type galaxies in MAnGA with IFU spectroscopy. We have seen that indeed velocity dispersions appear slightly larger at very low redshifts $z \lesssim 0.04$ than at $z \gtrsim 0.2$ for galaxies with $M_{\rm star} \sim 10^{11}\,{\rm M}_\odot$, but it is negligible for galaxies $M_{\rm star} \lesssim 3 \times 10^{10}\,{\rm M}_\odot$, in which instead the bias in velocity dispersion discussed above should be evident.

We also note that Kormendy (2019) does not mention the increasing sample of serendipitous local AGN, inclusive of early- and late-type galaxies (e.g. Busch et al. 2016; Reines & Volonteri 2015; Baron & Ménard 2019), that tend to lie up to an order of magnitude below the $M_{\rm bh}$–$M_{\rm star}$ relation of inactive, dynamically measured local black holes, providing further, independent evidence of the bias in the latter sample (Shankar et al. 2019b).

We conclude that the bias in black hole scaling relations that we infer in this paper (and our previous papers) is consistent with the data presented by Kormendy (2019).

[1]*Department of Physics and Astronomy, University of Southampton, Highfield SO17 1BJ, UK*

[2]*Department of Astronomy and the Center for Cosmology and Astroparticle Physics, The Ohio State University, 140 West 18th Avenue, Columbus OH 43210, USA*

[3]*Department of Physics and Astronomy, University of Pennsylvania, 209 South 33rd Str, Philadelphia, PA 19104, USA*

[4]*Department of Physics and Astronomy, Texas A&M University, College Station, TX 77843, USA*

[5]*Universitäts-Sternwarte, Ludwig-Maximilians-Universität München, Scheinerstr. 1, D-81679 München, Germany*

[6]*Instituto de Física y Astronomía, Universidad de Valparaíso, Gran Bretaa 1111, Playa Ancha, Valparaíso, Chile*

[7]*Centre for Extragalactic Astronomy, Department of Physics, Durham University, South Road, Durham DH1 3LE, UK*

[8]*Scuola Normale Superiore, Piazza dei Cavalieri 7, I-56126 Pisa, Italy*

[9]*Department of Physics, Yale University, PO Box 201820, New Haven, CT 06520, USA*

[10]*INAF Osservatorio Astronomico di Roma, via Frascati 33, I-00078 Monteporzio Catone, Italy*

[11]*INAF Osservatorio Astronomico di Trieste, Via Tiepolo 11, I-34131 Trieste, Italy*

[12]*Harvard-Smithsonian Center for Astrophysics, Cambridge, MA 02138, USA*

[13]*CEA, IRFU, DAp, AIM, Université Paris-Saclay, Université Paris Diderot, Sorbonne Paris Cité, CNRS, F-91191 Gif-sur-Yvette, France*

[14]*INAF Osservatorio Astronomico di Brera, Via Brera 28, I-20121 Milano, Italy*

[15]*Dipartimento di Matematica e Fisica, Università Roma Tre, via della Vasca Navale 84, I-00146 Roma, Italy*

[16]*SISSA, Via Bonomea 265, I-34136 Trieste, Italy*

[17]*National Astronomical Observatories, Chinese Academy of Sciences, Beijing 100101, People's Republic of China*

[18]*Institute of Space Sciences (ICE, CSIC), Campus UAB, Carrer de Magrans, E-08193 Barcelona, Spain*

[19]*Instituto de Astrofísica and Centro de Astroingeniería, Facultad de Física, Pontificia Universidad Católica de Chile, Casilla 306, Santiago 22, Chile*

[20]*University of Padova, Physics and Astronomy Department, Vicolo Osservatorio 3, I-35122 Padova, Italy*

[21]*Subaru Telescope, National Astronomical Observatory of Japan (NAOJ), 650 North Aohoku place, Hilo, HI 96720, USA*

[22]*Department of Physics, University of Bath, Claverton Down, BA2 7AY Bath, UK*

This paper has been typeset from a TeX/LaTeX file prepared by the author.